Oxy-functionalization of olefins with neat and heterogenized binuclear V (IV)O and Fe(II) complexes: Effect of steric hindrance on product selectivity and output in homogeneous and heterogeneous phase

Digvijaysinh K. Parmar[a], Pinal M. Butani[b], Niraj J. Thumar[b], Pinal M. Jasani[b], Ravi V. Padaliya[b], Paba R. Sandhiya[b], Haresh D. Nakum[c], Md. Nasim Khan[d], Dipak Makwana[e]

[a] Diu College, DHES, Diu (U.T.), 362520, India
[b] Department of Chemistry, School of Science, RK University, Rajkot 360020, Gujarat, India
[c] Oil and natural gas corporation limited, Hazira, Surat, Gujarat, India
[d] School of Chemistry, Cardiff University, Cardiff CF10 3AT, UK
[e] Inorganic Materials and Catalysis Division, CSIR-Central Salt and Marine Chemicals Research Institute, Bhavnagar 364002, Gujarat, India

ARTICLE INFO

Keywords:
Binuclear complex
Zeolite-Y
Olefin oxidation
Steric hindrance

ABSTRACT

Neat {[VO(sal2bz)]2; [Fe(sal2bz)(H2O)2]2·2H2O} and zeolite-Y immobilized {[VO(sal2bz)]2-Y; [Fe(sal2bz) (H2O)2]2-Y} binuclear complexes have been prepared and characterized by spectroscopic techniques (IR, UV–vis), elemental analyses (CHN, ICP-OES), thermal study (TGA), scanning electron micrograph (SEM), ad-sorption study (BET) and X-ray diffraction (XRD) patterns. Neat (homogeneous) and immobilized (hetero-geneous) complexes were employed as catalysts in the oxidation of olefins, namely, cyclohexene, limonene and α-pinene in the presence of 30% hydrogen peroxide. 100% conversion of cyclohexene and α-pinene was ob-tained while limonene was oxidized up to 90%. Homogeneous catalysts showed highly selective result as neat [VO(sal2bz)]2 complex has provided 87% cyclohexane-1,2-diol and neat [Fe(sal2bz)(H2O)2]2·2H2O complex has provided 79% verbenone in oxidation of cyclohexene and α-pinene, respectively. We have observed that due to steric hindrance, formation of olefinic oxidation products increases on moving from α-pinene to limonene and limonene to cyclohexene. Additionally. recovered heterogeneous catalysts showed intact results up to two consecutive runs. Probable catalytic mechanism has been proposed for oxidation of cyclohexene.

1. Introduction

Framework of zeolites is formed by an array of the corner-sharing AlO_4 or SiO_4 tetrahedra [1–3]. Periodic arrangement of these building blocks forms micropores of very regular dimensions. Micropores of the zeolites are accessible as they allow the diffusion of molecules through them. It makes zeolites at the top of the list of solids exhibiting huge surface areas, typically above 300 $m^2\ g^{-1}$ with an inner pore volume above 0.1 $cm^3\ g^{-1}$ [4].

In recent time, the meadow of inclusion materials has pulled up as eco-sustainable catalytic systems transforming various organic sub-strates into valuable intermediates for environmentally benign in-dustrial process [5–10]. Amongst the various type of modified micro-porous materials [11–18], zeolite-Y immobilized metal complexes occupy a special place in catalysis. Starting from the preparation of ship in bottle complexes, various complexes have been immobilized in zeolite-Y due to its structural diversity, redox behaviour [19–23] and possess potentials such as, thermal stability, reactivity, recyclability, and reusability [24] over homogeneous counterparts. Moreover, flex-ibility of Schiff base ligands has given direction to produce various zeolite-Y immobilized metal complexes as heterogeneous catalysts for organic transformation [25–27].

Oxy-functionalized derivatives of cyclic olefins are used in the preparation of several industrially important products [28–32]. Oxi-dation of olefinic positions provides epoxides and diols when high-va-lent metal oxo complexes are involved, whereas allylic oxidation results in allylic alcohols and ketones when one-electron processes or radical intermediates are involved [33]. Generally, the oxidation of olefins leads to a mixture of both the olefinic and allylic products. Therefore, it is a challenging task to achieve selectivity among olefinic and allylic products.

Herein we report the oxidation of olefins by using neat and zeolite-Y

Corresponding author.
E-mail address: parmardk@outlook.com (D.K. Parmar).

Table 1
Chemical composition of Schiff base ligand and neat complexes.

Entry	Material	Elements found (calculated) (%)				
		C	H	N	M	C/N
1	sal_2bzH_2	79.61 (79.57)	5.17 (5.14)	7.13 (7.14)	–	11.16 (11.14)
2	$[VO(sal_2bz)]_2$	67.16 (68.28)	3.84 (3.97)	6.00 (6.12)	10.82 (11.14)	11.19 (11.15)
3	$[Fe(sal_2bz)(H_2O)_2]_2 \cdot 2H_2O$	62.37 (62.42)	4.54 (4.83)	5.60 (5.60)	11.27 (11.16)	11.13 (11.14)

immobilized binuclear V(IV)O and Fe(II) complexes as catalysts to check their output in homogeneous and heterogeneous catalytic system, respectively.

2. Experimental section

2.1. Materials

Benzidine, 2-hydroxybenzaldehyde, DMF, 1,4-dioxane, acetonitrile, $VOSO_4 \cdot 5H_2O$, $FeSO_4 \cdot 7H_2O$, 30% H_2O_2, cyclohexene, limonene, α-pinene and zeolite-Y (Si/Al = 2.60) of AR grade were purchased from Hi-media (India) and used without further purification.

2.2. Preparation of ligand 'sal_2bzH_2'

Schiff base ligand (Z)-2-[4′-Methyleneamino-biphenyl-4-ylimino)-methyl]-phenol (sal_2bzH_2) was prepared by heating a mixture of ben-zidine (1.84 g, 10 mmol) with salicylaldehyde (2.13 mL, 20 mmol) in DMF medium under reflux condition with constant stirring for 4 h (see supplementary material, Scheme S1) [34]. The golden yellow solid product obtained was filtered off at room temperature and dried. sal_2bzH_2: Yellow crystals; m.p. > 250 °C; ^{1}H NMR (DMSO d_6, 400 MHz), δ: 13.08 (s, 1H, Ar-OH); 9.05 (s, 1H, Ar-OH); 7.95–6.99 (m, 16H, Ar-H); 6.65 (d, 1H, HC = N); 5.25 (d, 1H, HC = N) ppm (see supplementary material, Fig. S1).

2.3. Preparation of neat complexes

Aqueous solution of $VOSO_4 \cdot 5H_2O$ (1.26 g, 5 mmol) and $FeSO_4 \cdot 7H_2O$ (1.39 g, 5 mmol) was mixed separately with the solution of ligand sal_2bzH_2 (1.96 g, 5 mmol) in 1,4-dioxane with constant stirring (see supplementary material, Scheme S2). pH of the solution was adjusted around 5–6 by addition of CH_3COONa. The resulting solution was re-fluxed at 110 °C for 4–5 h. The mixture was cooled, filtered, washed and dried to obtain neat $[VO(sal_2bz)]_2$ and $[Fe(sal_2bz)(H_2O)_2]_2 \cdot 2H_2O$ com-plexes.

2.4. Preparation of zeolite-Y immobilized binuclear V(IV)O and Fe(II) complexes

Preparation of $[VO(sal_2bz)]_2$-Y and $[Fe(sal_2bz)(H_2O)_2]_2$-Y was done by Flexible Ligand method (see supplementary material, Scheme S3) [35]. Initially, V(IV)O and Fe(II) ions were incorporated separately in zeolite-Y through ion exchange method to prepare V(IV)O-Y and Fe(II)-Y. 1.0 g activated V(IV)O-Y and Fe(II)-Y was added separately to a so-lution of ligand sal_2bzH_2 in 1,4-dioxane (50 mL). The resulting mixture was heated at reflux condition with continuous stirring for 12 h, which gives immobilized binuclear V(IV)O and Fe(II) complexes. Soxhlet ex-traction was performed with 1,4-dioxane and acetonitrile solvent to remove complex or ligand adsorbed on the outer surface of zeolite. The resulting catalysts were named as $[VO(sal_2bz)]_2$-Y and $[Fe(sal_2bz)\ (H_2O)_2]_2$-Y.

2.5. Characterization of catalysts

CHN analysis was carried out on Perkin Elmer, USA 2400-II CHN analyzer. Percentage of Na(I), Al(III), Si(IV), V(IV)O and Fe(II) ions were checked by ICP-OES using Perkin Elmer optima 2000 DV model. BET analysis was done using ASAP 2010, micromeritics surface area analyser. SEM images were taken on LEO 1430 VP. Powder XRD pat-terns were recorded on Bruker AXS D_8 Advance X-ray powder dif-fractometer with a CuKα radiation as the incident beam. TGA was carried out using Perkin Elmer equipment and with the heating rate of 10 K/min. FT-IR spectra (4000–400 cm^{-1}) were recorded on a Thermo Nicolet FT-IR spectrometer in KBr. Magnetic property was measured by the magnetic susceptibility balance (Johnson Metthey and Sherwood model). UV–vis spectra were recorded on a Shimadzu UV-1800 spec-trophotometer, using a quartz cell of 1 cm^3 optical path. Reaction products were identified using GC–MS having a DB-5 capillary column (30 m ×0.30 mm ×0.25 μm) 95% silicoxane surface and FID detector. Area % method was used to quantify the products.

2.6. Catalytic oxidation reactions

The catalytic oxidation of cyclohexene, limonene and α-pinene were carried out by taking 10 mmol of substrate and 15 mg of catalyst in the acetonitrile medium. Meanwhile, 20 mmol of 30% H_2O_2 was added dropwise with constant stirring. The resulted reaction mixtures were heated at 80 °C for 24 h. Inspection of reaction progress and identifi-cation of products were carried out by GC-MS.

3. Results and discussion

3.1. Characterization

3.1.1. Chemical analysis data

As per the CHN analysis data, neat complexes (Table 1, entries 2 & 3) resulting from ligand sal_2bzH_2 (Table 1, entry 1) are formed by co-ordination with metal in 1:1 (metal:ligand) molar ratios. CHN data of zeolite-Y immobilized binuclear complexes (Table 2, entries 4 & 5) shows C/N ratio almost comparable with respect to neat complexes (Table 1, entries 2 & 3). It confirms the presence of binuclear complexes in framework of zeolite-Y [36].

Content of Al(III) and Si(IV) in the metal exchanged zeolite-Y (Table 2, entries 2 & 3) and immobilized complexes (Table 2, entries 4 & 5) are almost in the equivalent ratio with respect to pure zeolite-Y (Table 2, entry 1). It supports de-alumination in the framework of zeolite-Y during the metal ion exchange and complex formation. Low concentration of V(IV)O and Fe(II) ions in immobilized complexes than their respective metal exchanged zeolite-Y is owing to leaching of metal ions during the immobilization [37].

Table 2
Chemical composition of zeolite-Y and zeolite-Y modified materials.

Entry	Material	Elements found (%)						
		C	N	M	C/N	Si	Al	Si/Al
1	Na-Y	–	–	–	–	17.04	6.54	2.60
2	V(IV)O-Y	–	–	0.59	–	16.52	6.36	2.59
3	Fe(II)-Y	–	–	0.63	–	16.57	6.37	2.60
4	$[VO(sal_2bz)]_2$-Y	1.01	0.09	0.34	11.22	16.23	6.24	2.60
5	$[Fe(sal_2bz)(H_2O)_2]_2$-Y	1.90	0.17	0.41	11.17	16.10	6.19	2.60

Table 3
BET analysis data of zeolite-Y and zeolite-Y modified materials.

Entry	Material	BET surface area ($m^2\ g^{-1}$)	Pore volume ($cm^3\ g^{-1}$)	(%)[a]	(%)[b]
1	Na-Y	627	0.309	–	–
2	V(IV)O-Y	541	0.234	24.2	–
3	Fe(II)-Y	532	0.276	10.6	–
4	[VO(sal$_2$bz)]$_2$-Y	156	0.104	66.3	55.5
5	[Fe(sal$_2$bz)(H$_2$O)$_2$]$_2$-Y	223	0.120	61.2	56.5

[a] Reduction in pore volume compared to Na-Y.
[b] Reduction in pore volume compared to M(II)-Y.

3.1.2. BET analysis

BET data reveal that zeolite-Y possess 627 $m^2\ g^{-1}$ surface area and 0.309 $cm^3\ g^{-1}$ pore volume (Table 3, entry 1) [38]. The immobilization of metal ions and complex reduces the available pore volume which leads to decrease in adsorption ability of zeolitic pores. Mainly, it de-pends on the geometry of immobilized complex in framework of zeolite-Y. BET surface area and pore volume of immobilized complexes (Table 3, entries 4 & 5) gets reduced to ~55% upon immobilization with respect to their respective metal exchanged zeolite-Y (Table 3, entries 2 & 3). The falling in the value clearly suggest the presence of complex within the zeolite-Y cavities [39].

3.1.3. Powder XRD study

Except a slight change in the peak intensity, there are no major differences in XRD patterns of M(II)-Y and immobilized complexes while comparing them with XRD patterns of zeolite-Y (see supple-mentary material, Fig. S2) [40]. The intensities of the 3 1 1 and 2 2 0 in zeolite-Y, that is, $I_{2\,2\,0} > I_{3\,1\,1}$, was varied to $I_{3\,1\,1} > I_{2\,2\,0}$ in the case of XRD patterns of M(II)-Y and immobilized complexes. This variation is influenced by the immobiliztion of metal complex which leads to dis-turb the randomly distributed sodium ions of zeolite-Y framework. These remarks suggest that crystallinity of zeolite-Y remained intact even after immobilization process [41].

3.1.4. SEM analysis

Soxhlet extraction was carried out to remove the ligand or metal complex adsorbed on the external surface of zeolite-Y [42]. To confirm the removal of exraneous particles, SEM images of [VO(sal$_2$bz)]$_2$-Y were taken before and after Soxhlet extraction process (see supplementary material, Fig. S3).

3.1.5. FT-IR study

The FT-IR spectra of ligand sal$_2$bzH$_2$ as well as neat and immobilized binuclear complexes have been studied to characterize their structures (see supplementary material, Fig. S4). As per the data given in Table 4, a band at ~1045 cm^{-1} seen in immobilized complexes (Table 4, entries 4 & 5) is corresponding to the asymmetric stretching vibrations of SiO_4/ AlO_4 units [43]. Most of the bands of zeolite framework found around 1193, 827 and 451 cm^{-1} [44].

Ligand sal$_2$bzH$_2$ shows a band at 1616 cm^{-1} is corresponding to ν(C]N). Neat V(IV)O and Fe(II) complexes (Table 4, entries 2 & 3) show bands at 1612 cm^{-1} and 1596 cm^{-1}, respectively, are corre-sponding to $\nu_{(C=N)}$ group [45]. It confirms the coordination of metal ions with azomethine nitrogen. Moreover, this band also found in both immobilized complexes.

Moreover, $\nu_{(CeO)}$ band for both neat complexes shifted towards lower frequency with respect to $\nu_{(C-O)}$ band of free ligand sal$_2$bzH$_2$, which indicates the coordination of metal ions with oxygen atom [46].
A broadband around ~3200-3400 cm^{-1}, and two weaker bands around 827 cm^{-1} and 601 cm^{-1} in zeolite-Y immobilized complexes are at-tributed to −OH stretching, rocking and wagging vibrations, respec-tively [47]. Absence of $\nu_{(OeH)}$ in neat V(IV)O complex is due to the absence of water molecule in the coordination sphere. Moreover, $\nu_{(V]O)}$ vibration in neat V(IV)O complex is found at 977 cm^{-1} which indicates the absence of intermolecular V]O···V]O bonding. How-ever, $\nu_{(V]O)}$ vibration is missing in zeolite-Y immobilized V(IV)O complex due to the overlapping with zeolitic vibration.

3.1.6. UV–vis study and magnetic property

Electronic spectra of ligand sal$_2$bzH$_2$ and neat binuclear complexes of V(IV)O and Fe(II) were taken in DMSO, while of zeolite-Y and im-mobilized binuclear complexes were taken in diluted HF solution. The free ligand sal$_2$bzH$_2$ (Table 5, entry 1) exhibit three bands at 240, 294, and 364 nm due to ILCT, π → π* (aromatic moiety) and n → π* (C]N chromophore) transitions, respectively [48].

As per the data, spectra of neat V(IV)O complex (Table 5, entry 2) showed strong bands at 286 and 370 nm are corresponding to π → π* transition and charge transfer transition, respectively. It also shows weak bands at 418, 532 and 620 nm due to d-d transition. It suggests the square-pyramidal geometry V(IV)O complex [49]. The bands at 291, 361 and 769 nm in case of neat [Fe(sal$_2$bz)(H$_2$O)$_2$]$_2$ ·2H$_2$O complex (Table 5, entry 3) are attributable to π → π*, charge transfer and d-d transition, respectively. It recommends the octahedral environment around the Fe(II) [50].

Dehydrated zeolite-Y (Table 5, entry 4) displays an intense band at 306 nm due to charge transfer transition for oxygen to aluminium atoms of two different Al-O units present in zeolite-Y [51]. Zeolite-Y immobilized binuclear V(IV)O and Fe(II) complexes (Table 5, entries 5 & 6) also shows d-d transition, which suggest the presence of complex within zeolite-Y.

The magnetic moment of the neat V(IV)O complex is found to be 1.59 B.M at room temperature which is quite less than that of V(IV)O monomer complexes. The lower magnetic moment of this dimer com-plex is due to magnetically dilute nature of the complexes in which the one metal ion is not involved in magnetic exchange (due to no bridging ligand between two metal centres) with the neighbouring metal ions [52]. The V(IV)O complexes of the magnetically dilute complexes should record magnetic moments very close to the spin-only value when the orbital contribution is completely quenched. However, if the orbital contribution is not completely quenched the magnetically dilute V(IV)O complexes may exhibit magnetic moments even less than the spin-only (1.73 BM) value [53,54].

3.1.7. TGA study

Thermal degradation of neat V(IV)O complex (Table 6, entry 1) took place in two stages. The first decomposition stage in the range of

Table 4
FTIR spectral data of zeolite-Y and prepared materials.

Entry	Material	Internal vibrations			External vibrations			$\nu_{(V=O)}$	$\nu_{(C=N)}$	$\nu_{(C-O)}$	$\nu_{(O-H)}$
		ν_{asym} T-O	ν_{sym} T-O	ν_{bend} T-O	D-R	ν_{sym} T-O	ν_{asym} T-O				
1	sal$_2$bzH$_2$	–	–	–	–	–	–	–	1616	1097	3050
2	[VO(sal$_2$bz)]$_2$	–	–	–	–	–	–	977	1612	1087	–
3	[Fe(sal$_2$bz)(H$_2$O)$_2$]$_2$·2H$_2$O	–	–	–	–	–	–	–	1596	1062	3319
4	[VO(sal$_2$bz)]$_2$-Y	1045	599	447	514	827	1192	–	1608	1140	3480
5	[Fe(sal$_2$bz)(H$_2$O)$_2$]$_2$-Y	1045	601	451	574	827	1170	–	1610	1193	3470

Table 5
UV–vis spectral data of zeolite-Y and zeolite-Y modified materials.

Entry	Material	Electronic transition (nm)			
		π-π* (strong)	n-π* (weak)	CT (strong)	d-d (weak)
1	sal_2bzH_2	240, 294	364	–	–
2	$[VO(sal_2bz)]_2$	286	302	370	418, 532, 620
3	$[Fe(sal_2bz)(H_2O)_2]_2 \cdot 2H_2O$	291	306	361	769
4	Na-Y	–	–	306	–
5	$[VO(sal_2bz)]_2$-Y	218, 254, 281	306	374	418, 527, 624
6	$[Fe(sal_2bz)(H_2O)_2]_2$-Y	206, 267	321	365	752

Table 6
TGA data of prepared materials.

Entry	Material	T range (°C)	Weight loss (%)	Group loss
1	$[VO(sal_2bz)]_2$	280-350	78.18	Ligand
		550-700	21.92	V_2O_3 residue
2	$[Fe(sal_2bz)$	80-250	9.69	H_2O
	$(H_2O)_2]_2 \cdot 2H_2O$	280-350	74.13	Ligand
		550-700	16.28	Fe_2O_3 residue
3	Na-Y	30-120	11.84	H_2O
4	$[VO(sal_2bz)]_2$-Y	80-120	4.61	H_2O
		450-700	12.97	Decomposition of complex
5	$[Fe(sal_2bz)(H_2O)_2]_2$-Y	80-250	5.47	H_2O
		480-700	14.51	Decomposition of complex

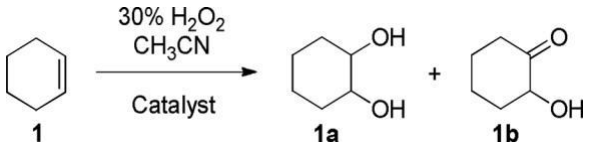

Scheme 1. Catalytic oxidation of cyclohexene.

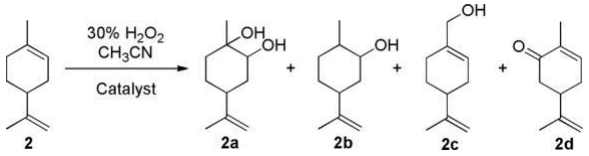

Scheme 2. Catalytic oxidation of limonene.

280–350 °C is corresponding to the loss of ligand sal_2bzH_2, with 78.18% mass loss. The final residues were estimated as vanadium oxide. Decomposition of neat Fe(II) complex (Table 6, entry 2) fall in three stages. The first decomposition stage involves loss of hydrated and coordinated H_2O molecules in the range of 80–250 °C. Further, loss of ligand sal_2bzH_2 take place in the range of 280–350 °C with mass loss of 74.13% and leaving the residue of iron oxide.

Degradation of zeolite-Y (Table 6, entry 3) about 11.84% was found within 30–120 °C due the loss of free intra zeolite H_2O molecules [55]. The first decomposition stage of zeolite-Y immobilized binuclear com-plexes (Table 6, entries 4 & 5) falls in the range of 80–250 °C. It is due to removal of intrazeolite and coordinated H_2O molecules. The second decomposition stage involves ~13% mass loss around 480 °C due to the degradation of metal complex.

3.2. Catalytic activity

3.2.1. Oxidation of cyclohexene

In present study, 100% conversion of cyclohexene (1) was achieved (Table 7, entries 1–4). The catalyzed oxidation of cyclohexene gave mainly two products, that is, cyclohexane-1,2-diol (1a) and 2-hydroxy cyclohexanone (1b) as shown in Scheme 1 [(see supplementary mate-rial, Fig. S5 (a & b)].

The formation of water due to the decomposition of H_2O_2 is somehow responsible for the hydrolysis of cyclohexene oxide to 1a. Other products (formation of 1b through further oxidation of 1a) found in relatively low amounts in this reaction. The formation of the olefinic oxidation products reflects the attack over the double bond of cyclo-hexene [56]. The selectivity of the products follows the order: 1a > 1b. The percentage of product selectivity is different in case of neat and immobilized complexes. Among the catalysts used, neat $[VO(sal_2bz)]_2$ (Table 7, entry 3) showed higher selectivity by providing 87% 1a, while immobilized $[VO(sal_2bz)]_2$-Y (Table 7, entry 4) showed 70% selectivity of 1a. On the other hand, immobilized $[VO(sal_2bz)]_2$-Y showed 9989 TON, while $[VO(sal_2bz)]_2$ displayed only 314 TON.

3.2.2. Oxidation of limonene

As displayed in Scheme 2, prepared catalysts also catalyzed the oxidation of limonene (2) by 30% H_2O_2 to give limonene glycol (2a), dihydro-carveol (2b), (S)-perillyl alcohol (2c), and carvone (2d) [see supplementary material, Fig. S6 (a, b, c & d)]. Amongst the catalysts

Table 7
Catalytic activity of prepared materials over oxidation of cyclohexene[a].

Entry	Catalyst	Conversion (%)	Olefinic product (%)		Other product (%)	Metal (μmol) in catalyst[b]	TON[c]
			1a	1b			
1	$[Fe(sal_2bz)(H_2O)_2]_2 \cdot 2H_2O$	100	54	10	36	30.2	331
2	$[Fe(sal_2bz)(H_2O)_2]_2$-Y	100	50	12	38	1.10	9090
3	$[VO(sal_2bz)]_2$	100	87	7	6	31.8	314
4	$[VO(sal_2bz)]_2$-Y	100	70	10	20	1.00	10000
5	$[VO(sal_2bz)]_2$-Y[d]	96	69	11	20	1.00	9600
6	$[VO(sal_2bz)]_2$-Y[e]	95	70	10	19	1.00	9500

[a] Reaction conditions: 10 mmol (1.01 mL) cyclohexene, 20 mmol (2.03 mL) 30% H_2O_2, 15 mg catalyst, 3 mL acetonitrile, 80 °C, 24 h.
[b] Amount of metal (μmol) present per 15 mg of catalyst.
[c] TON: Turnover number = mol of cyclohexene converted/mol of M(II).
[d] First reuse of catalyst.
[e] Second reuse of catalyst.

Table 8

Catalytic activity of prepared materials over oxidation of limonene[a].

Entry	Catalyst	Conversion (%)	Olefinic product (%)		Allylic product (%)		Other product (%)	Metal (μmol) in catalyst[b]	TON[c]
			2a	2b	2c	2d			
1	$[Fe(sal_2bz)(H_2O)_2]_2{\cdot}2H_2O$	79	52	13	15	10	10	30.2	262
2	$[Fe(sal_2bz)(H_2O)_2]_2$-Y	80	43	17	15	14	11	1.10	7272
3	$[VO(sal_2bz)]_2$	84	43	18	14	14	11	31.8	264
4	$[VO(sal_2bz)]_2$-Y	90	39	20	17	12	12	1.00	9000
5	$[VO(sal_2bz)]_2$-Y[d]	87	40	18	16	14	12	1.00	8700
6	$[VO(sal_2bz)]_2$-Y[e]	87	40	18	16	12	14	1.00	8700

[a] Reaction conditions: 10 mmol (1.61 mL) limonene, 20 mmol (2.03 mL) 30% H_2O_2, 15 mg catalyst, 3 mL acetonitrile, 80 °C, 24 h.

[b] Amount of metal (μmol) present per 15 mg of catalyst.

[c] TON: Turnover number = mol of limonene converted/mol of M(II).

[d] First reuse of catalyst.

[e] Second reuse of catalyst.

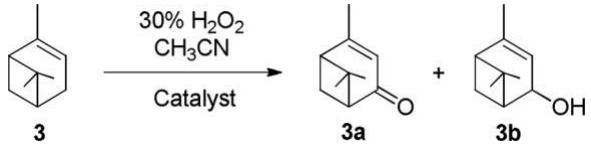

Scheme 3. Catalytic oxidation of α-pinene.

used, neat $[VO(sal_2bz)]_2$ complex has provided highest 84% conversion (Table 8, entry 3), while 90% conversion was achieved by immobilized $[VO(sal_2bz)]_2$-Y complex (Table 8, entry 4).

3.2.3. Oxidation of α-pinene

Catalyzed oxidation of α-pinene (3) mainly gave allylic products [57], that is, verbenone (3a) and verbenol (3b) (Scheme 3) [see sup-plementary material, Fig. S7 (a & b)]. The conversion of α-pinene and the selectivity of different reaction products are presented in Table 9. All catalysts were able to provide 100% conversion of α-pinene to oxy-functionalized products. Neat $[Fe(sal_2bz)(H_2O)_2]_2{\cdot}2H_2O$ demonstrated 79% selectivity of 3a, which is highest among the catalysts used. Though, selectivity percentage of the products differ in neat and re-spective immobilized complexes.

For recycling study, immobilized complexes were successfully re-covered after completion of reaction by simple filtration, washing with acetonitrile and drying at ca. 150 °C. Catalysts could be reused at least two times without loss of olefin conversion and product selectivity under similar reaction conditions (Table 7–9; entries 5 & 6).

Na-Y, V(IV)O-Y and Fe(II)-Y are unable to carry out oxidation of cyclohexene, limonene and α-pinene to their oxy-functionalized pro-ducts with greater amount [55,56]. In this study, both the neat and immobilized binuclear V(IV)O and Fe(II) complexes showed excellent conversion of cyclohexene (100%), α-pinene (100%) and limonene (90%). It proves that metal complex delivers the active site for the oxidation of olefins.

Though, both the homogeneous and heterogeneous catalysts have their own excellence and drawback. Here, homogeneous V(IV)O and Fe (II) catalysts have demonstrated good product selectivity while het-erogeneous V(IV)O and Fe(II) catalysts have provided better TON in olefins oxidation. On looking towards demerit, homogeneous catalysts suffering with separation problem as they were decomposed after first run while heterogeneous catalysts possess selectivity issues. The cata-lytic system (homogeneous and heterogeneous) for the oxidation of olefins studied previously is shown in Table 10.

Literature reports that temperature and steric hindrance are the factors that affect the selectivity among olefinic and allylic oxidation [71]. Allylic oxidative products predominate over olefinic products at higher temperature (above 40 °C). Though, in our case, despite of higher reaction temperature (80 °C), oxidation of cyclohexene provides major selectivity for olefinic oxidation and yields cyclohexane-1,2-diol after hydrolysis. It may be due to the flexible nature of cyclohexene with no such steric crowding makes free space available for active site to approach. Whereas, oxidation of α-pinene proceed via allylic route due to steric hindrance of rigid moiety which makes difficult for closet approach of active site towards C]C double bond.

Here, we have observed that steric hindrance decreases on moving from α-pinene to limonene and from limonene to cyclohexene. Subsequently, formation of olefinic oxidation products increases and of allylic products decreases (Scheme 4).

Catalytic oxidation of cyclohexene by $[VO(sal_2bz)]_2$ complex pro-ceeds via olefinic oxidation path as shown in Scheme 5. Initially, $[VO(sal_2bz)]_2$ (A) interacts with H_2O_2 to form metal peroxo species which further undergoes homolytic cleavage to give product (B). Oxidative addition of product (B) to the C]C of cyclohexene gives intermediate (C) which undergoes migratory insertion to give cyclohexene epoxide

Table 9

Catalytic activity of prepared materials over oxidation of α-pinene[a].

Entry	Catalyst	Conversion (%)	Allylic product (%)		Other product (%)	Metal (μmol) in catalyst[b]	TON[c]
			3a	3b			
1	$[VO(sal_2bz)]_2$	100	54	15	32	31.8	314
2	$[VO(sal_2bz)]_2$-Y	100	40	30	30	1.00	10000
3	$[Fe(sal_2bz)(H_2O)_2]_2{\cdot}2H_2O$	100	79	11	10	30.2	331
4	$[Fe(sal_2bz)(H_2O)_2]_2$-Y	100	46	34	20	1.10	9090
5	$[Fe(sal_2bz)(H_2O)_2]_2$-Y[d]	98	43	34	23	1.10	8909
6	$[Fe(sal_2bz)(H_2O)_2]_2$-Y[e]	98	43	35	22	1.10	8909

[a] Reaction conditions: 10 mmol (1.58 mL) α-pinene, 20 mmol (2.03 mL) 30% H_2O_2, 15 mg catalyst, 3 mL acetonitrile, 80 °C, 24 h.

[b] Amount of metal (μmol) present per 15 mg of catalyst.

[c] TON: Turnover number = mol of α-pinene converted/mol of M(II).

[d] First reuse of catalyst.

[e] Second reuse of catalyst.

Table 10
Comparison of reported homogeneous and heterogeneous catalytic systems with present study over oxidation of olefins 1, 2 and 3.

Sr. No.	Olefin	Homogeneous catalyst /oxidant; Heterogeneous catalyst /oxidant	Conversion (%)*	TON[a]	Selectivity[b] (%)*		Ref
1	1	$[VO(sal_2bz)]_2$ /H_2O_2	100	314	Cydiol (87)	Hycyone (13)	This study
		$[VO(sal_2bz)]_2$-Y /H_2O_2	100	9989	Cydiol (70)	Hycyone (10)	This study
2	1	[VO(hacen)] /H_2O_2	96	–	Cyone (49)	Cyol (48)	[58]
		[VO(hacen)]-Y /H_2O_2	100	–	Cyone (37)	Cyol (49)	[58]
3	1	$[VO(L^1)(acac)]$ /H_2O_2	87	–	Cyol (46)	Cyox (28)	[59]
		$[VO(L^1)(acac)]$-Y /H_2O_2	75	–	Cyone (48)	Cyox (25)	[59]
4	1	$[VO(tmbmz)_2]$ /H_2O_2	64	–	Cydiol (85)	Cyone (12)	[60]
		PS-$[VO(ligand)_n]$ /H_2O_2	86	–	Cydiol (81)	Cyone (15)	[60]
5	1	$[V^{IV}O(acac)(pydx\text{-}aepy)]$ /H_2O_2	82	–	Cyone (45)	Cyol (33)	[61]
		$[V^{V}O_2(pydx\text{-}aepy)]$-Y /$H_2O_2$	99	–	Cyone (~50)	Cyol (~35)	[61]
6	1	3 /H_2O_2	71	–	Cyol (51)	Cyone (48)	[62]
		3Y /H_2O_2	99	–	Cyol (39)	Cyone (56)	[62]
7	1	$[V^{IV}O(fsal\text{-}DL\text{-}Ala)(H_2O)]$ /H_2O_2	54	–	Cyol (53)	Cyox (39)	[63]
		PS-$[V^{IV}O(fsal\text{-}DL\text{-}Ala)(H_2O)]$ /H_2O_2	79	–	Cyol (48)	Cyox (35)	[63]
8	1	$[V^{IV}O(pydx\text{-}1,3\text{-}pn)]$ /H_2O_2	32	–	Cyol (57)	Cyone (32)	[64]
		$[V^{IV}O(pydx\text{-}1,3\text{-}pn)]$-Y /$H_2O_2$	93	–	Cyol (44)	Cyone (47)	[64]
9	2	$[VO(sal_2bz)]_2$ /H_2O_2	84	262	Lgly (36)	Pal (6)	This study
		$[VO(sal_2bz)]_2$-Y /H_2O_2	90	9020	Lgly (35)	Pal (4)	This study
10	2	$[VO(VTCH)_2]$ /TBHP	86	–	Lgly (34)	Col (10)	[65]
		$[VO(VTCH)_2]$-Y /TBHP	98	–	Lgly (45)	Col (8)	[65]
11	2	5 /H_2O_2	97	50	Cone (70)	Col (17)	[66]
		5Y /H_2O_2	82	2273	Cone (78)	Col (11)	[66]
12	2	$[Fe(L)_2(H_2O)_2]\cdot 2H_2O$ /H_2O_2	66	205	Cone (63)	Col (17)	[67]
		$[Fe(L)_2(H_2O)_2]$-Y /H_2O_2	79	2372	Cone (71)	Col (14)	[67]
13	2	$[VO(L)\cdot H_2O]$ /H_2O_2	51	–	Cone (39)	Col (20)	[68]
		$[VO(L)\cdot H_2O]$-Y /H_2O_2	87	–	Cone (41)	Col (32)	[68]
14	3	$[Fe(sal_2bz)(H_2O)_2]_2\cdot 2H_2O$ /H_2O_2	100	349	Vone (79)	Vol (11)	This study
		$[Fe(sal_2bz)(H_2O)_2]_2$-Y /H_2O_2	100	9082	Vone (46)	Vol (34)	This study
15	3	5 /H_2O_2	81	–	Vone (77)	Vol (11)	[66]
		5Y /H_2O_2	73	–	Vone (73)	Vol (12)	[66]
16	3	$[Fe(L)_2(H_2O)_2]\cdot 2H_2O$ /H_2O_2	59	183	Vone (59)	Vol (14)	[67]
		$[Fe(L)_2(H_2O)_2]$-Y /H_2O_2	67	2012	Vone (64)	Vol (19)	[67]
17	3	$VOJL_2$ /TBHP	40	47	Vone (44)	Vol (39)	[69]
		$VOJL_2$-Y /TBHP	45	598	Vone (41)	Vol (42)	[69]
18	3	Fe_3O_4 /O_2	5	–	Vol (40)	Vone (20)	[70]
		Co-Fe_3O_4 /O_2	36	100	Vol (40)	Piox (26)	[70]

[a] TON: Turn over number.

[b] Selectivity: Cydiol = Cyclohexane-1,2-diol; Hycyone = 2-hydroxy cyclohexanone; Cyox = Cyclohexene oxide; Cyol = 2-Cylohexen-1-ol; Cyone = 2-Cyclohexen-1-one; Lox = Limonene oxide; Lgly = Limonene glycol; Pal= (S)-Perillyl alcohol; Cone = Carvone; Col = Carveol; Vone = Verbenone; Vol = Verbenol; Piox = Pinene oxide.

* Conversion and selectivity % are rounded off.

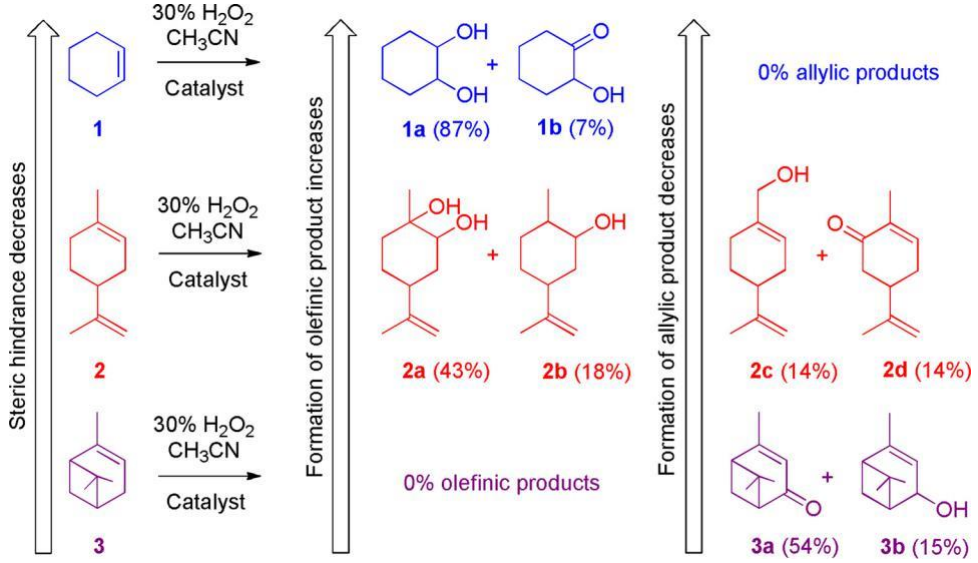

Scheme 4. Effect of steric hindrance on product selectivity.

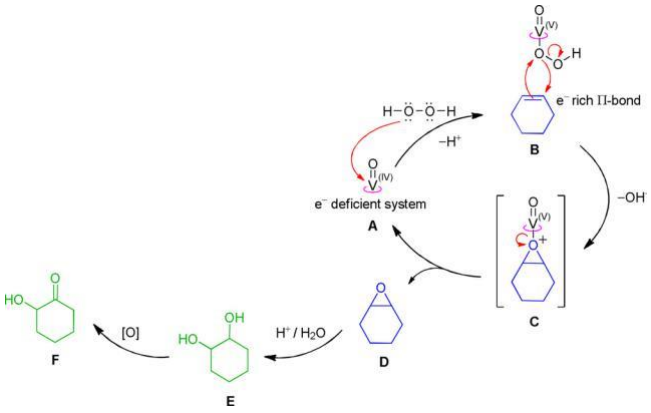

Scheme 5. Proposed mechanism for oxidation of cyclohexene by $[VO(sal_2bz)]_2$.

(D) and regenerates $[VO(sal_2bz)]_2$ (A). Furthermore, cyclohexene ep-oxide (D) undergoes in situ hydrolysis to produce cyclohexane-1,2-diol (E), which further oxidized to 2-hydroxy cyclohexanone (F).

4. Conclusions

As outlined, homogeneous and heterogeneous binuclear complexes of V(IV)O and Fe(II) were prepared and characterized. V(IV)O and Fe (II) complexes efficiently catalyzed the oxidation of olefins. In the oxidation of cyclohexene, 100% conversion was obtained by each cat-alyst and selectivity of the products varied in the order: cyclohexane-1,2-diol > 2-hydroxycyclohexanone. Conversion of limonene found in the order: $[VO(sal_2bz)]_2$-Y (90%) > $[VO(sal_2bz)]_2$ (84%) > $[Fe(sal_2bz)(H_2O)_2]_2$-Y (80%) > $[Fe(sal_2bz)(H_2O)_2]_2 \cdot 2H_2O$ (79%). While selectivity order of the two main products being: limonene glycol > (S)-perillyl alcohol. α-pinene was also oxidized completely (100%) by each catalyst and two reaction products with the selectivity order: verbenone > verbenol have been obtained during the oxidation.

Steric hindrance plays the major role in the selectivity of products as less hindered cyclohexene gave epoxide products and more hindered α-pinene provided allylic products. Almost similar results in recycling study proves the ability of solid support to prevent decomposition of complex during the reaction. While absence of metal leaching proves the heterogeneous character of immobilized catalysts. In contrast to homogeneous counterparts, advantage of being recyclable, reusable, and higher stability makes heterogeneous catalysts significantly more environmentally benign.

Acknowledgements

We thank School of Science, RK University, Rajkot, India for pro-viding laboratory and instrument facilities.

References

[1] J. Zhu, X. Meng, F. Xiao, Front. Chem. Sci. Eng. 7 (2013) 233–248.
[2] W.J. Roth, P. Nachtigall, R.E. Morris, J. Cejka, Chem. Rev. 114 (2014) 4807–4837.
[3] K. Na, G.A. Somorjai, Catal. Lett. 145 (2015) 193–213.
[4] International Zeolite Association Database, (2011) http://www.izastructure.org/databases.
[5] C. Teixeira, New J. Chem. 32 (2008) 2263–2269.
[6] Y.S. Park, J. Am. Chem. Soc. 124 (2002) 7123–7135.
[7] M.R. Maurya, U. Kumar, I. Correia, P. Adão, J.C. Pessoa, Eur. J. Inorg. Chem. 4 (2008) 577–587.
[8] A.R. Silva, H. Albuquerque, S. Borges, R. Siegel, L. Mafra, A.P. Carvalho, J. Pires, Microporous Mesoporous Mater. 158 (2012) 26–38.
[9] A. Corma, R.M. Martin-Aranda, J. Catal. 130 (1991) 130–137.
[10] T. Joseph, S.S. Deshpande, S.B. Halligudi, A. Vinu, S. Ernst, M. Hartmann, J. Mol. Catal. A Chem. 206 (2003) 13–21.
[11] J. Pérez-Ramírez, C.H. Christensen, K. Egeblad, C.H. Christensen, J.C. Groen, Chem. Soc. Rev. 37 (2008) 2530–2542.
[12] N. Pal, A. Bhaumik, Adv. Colloid Interface Sci. 189–190 (2013) 21–41.
[13] S. Lopez-Orozco, A. Inayat, A. Schwab, T. Selvam, W. Schwieger, Adv. Mater. 23 (2011) 2602–2615.
[14] A. Corma, Chem. Rev. 97 (1997) 2373–2420.
[15] A. Taguchi, F. Schüth, Microporous Mesoporous Mater. 77 (2005) 1–45.
[16] C. Perego, R. Millini, Chem. Soc. Rev. 42 (2013) 3956–3976.
[17] R.M. Martín-Aranda, J. Cejka, Top. Catal. 53 (2010) 141–153.
[18] S. Fujita, S. Inagaki, Chem. Mater. 20 (2008) 891–908.
[19] P.K. Dutta, J.A. Incavo, J. Phys. Chem. 91 (1987) 4443–4446.
[20] M. Salavati-Niasari, Chem. Lett. 34 (2005) 1444–1445.
[21] M. Salavati-Niasari, Mahnaz Dadkhah, Fatemeh Davar, Inorg. Chim. Acta Rev. 362 (2009) 3969–3974.
[22] M. Salavati-Niasari, Chem. Lett. 34 (2005) 244–245.
[23] M. Salavati-Niasari, Zohreh Salimi, Mahdi Bazarganipour, Fatemeh Davar, Inorg. Chim. Acta Rev. 362 (2009) 3715–3724.
[24] W.J. Roth, P. Nachtigall, R.E. Morris, J. Cejka, Chem. Rev. 114 (2014) 4807–4837.
[25] M. Salavati-Niasari, M. Shakouri-Arani, F. Davar, Microporous Mesoporous Mater. 116 (2008) 77–85.
[26] M.R. Maurya, A.K. Chandrakar, S. Chand, J. Mol. Catal. A Chem. 270 (2007) 225–235.
[27] B. Dutta, S. Jana, S. Bhunia, H. Honda, S. Koner, Appl. Catal. A Gen. 382 (2010) 90–98.
[28] M. Salavati-Niasari, Microporous Mesoporous Mater. 95 (2006) 248–256.
[29] P. Oliveira, M.L. Rojas-Cervantes, A.M. Ramos, I.M. Fonseca, A.M.B. Rego, J. Vital, Catal. Today 118 (2006) 307–314.
[30] B. Cornils, W.A. Herrmann, Applied Homogeneous Catalysis With Organometallic Compounds, second ed., Wiley-VCH, Weinheim, 2002, pp. 1–1383.
[31] M. Salavati-Niasari, P. Salemi, F. Davar, J. Mol. Catal. A Chem. 238 (2005) 215–222.
[32] M. Salavati-Niasari, J. Mol. Catal. A Chem. 229 (2005) 159–164.
[33] A.B. Sorokin, Chem. Rev. 113 (2013) 8152–8191.
[34] R.K. Al shemary, Z.A. Shafiq, Asian J. Pharm. Sci. Tech. 5 (2015) 172–178.
[35] F. Farzaneh, J. Soleimannejad, M. Ghandi, J. Mol. Catal. A Chem. 118 (1997) 223–227.
[36] T.A. Yousef, G.M. Abu El-Reash, O.A. El-Gammal, R.A. Bedier, J. Mol. Struct. 1035 (2013) 307–317.
[37] K.J. Balkus, A.G. Gabrielov, J. Incl. Phenom. Mol. Recognit. Chem. 21 (1995) 159–184.
[38] S.P. Varkey, C. Ratnasamy, P. Ratnasamy, J. Mol. Catal. A Chem. 135 (1998) 295–306.
[39] S.P. Varkey, C.R. Jacob, Indian J. Chem. 37A (1998) 407–412.
[40] W.H. Quayle, J.H. Lunsford, Inorg. Chem. 21 (1982) 97–103.
[41] C.K. Modi, N. Solanki, R. Vithalani, D. Patel, Appl. Organometal Chem. 32 (2017) 1–13.
[42] S.P. Varkey, C. Ratnasamy, P. Ratnasamy, J. Mol. Catal. A Chem. 135 (1998) 295–306.
[43] C.K. Modi, P.M. Trivedi, Adv. Mat. Lett. 3 (2012) 149–153.
[44] K.B. Kusum, C.D. Ramesh, J. Phys. Chem. C 116 (2012) 14295–14310.
[45] H.S. Abbo, S.J.J. Titinchi, Top. Catal. 53 (2010) 254–264.
[46] C.K. Modi, P.M. Trivedi, Microporous Mesoporous Mater. 155 (2012) 227–232.
[47] C.K. Modi, B.G. Gade, J.A. Chudasama, D.K. Parmar, H.D. Nakum, A.L. Patel, Spectrochim. Acta, Part A. 140 (2015) 174–184.
[48] J.P. Mehta, D.K. Parmar, H.D. Nakum, D.R. Godhani, N.C. Desai, J. Porous Mater. 23 (2016) 1507–1518.
[49] J.P. Mehta, D.K. Parmar, D.R. Godhani, H.D. Nakum, N.C. Desai, J. Mol. Catal. A Chem. 421 (2016) 178–188.
[50] J.C. Bailar, H.J. Emeleus, R. Nyholm, A.F. Trotman-Dickenson, Comprehensive Inorganic Chemistry, Pergamon Press, New York, 1973.
[51] R.K. Agarwal, I. Chakraborti, S.K. Sharma, Pol. J. Chem. 68 (1994) 1085–1092.
[52] A. Syamal, Coord. Chem. Rev. 16 (1975) 309–339.
[53] Y.A. Kasparova, V.V. Zelentsov, Zh. Strukt. Khim. 9 (1968) 532.
[54] T.D. Smith, T. Lund, J.R. Pilbrow, J.H. Price, J. Chem. Soc. A. (1971) 2936–2939.
[55] M.R. Maurya, S.J.J. Titinchi, S. Chand, Appl. Catal. A Gen. 228 (2002) 177–187.
[56] P.P. Knops-Gerrits, M. L'abbe, A. Jacobs, Epoxidation With Manganese N,N-bis(2-Pyridinecarboxamide) Complexes Encapsulated in Zeolite Y, Elsevier Science, Amsterdam, 1997, pp. 445–452.
[57] I.Y. Skobelev, A.B. Sorokin, K.A. Kovalenko, V.P. Fedin, O.A. Kholdeeva, J. Catal. 298 (2013) 61–69.
[58] D.R. Godhani, H.D. Nakum, D.K. Parmar, J.P. Mehta, N.C. Desai, J. Mol. Catal. A Chem. 415 (2016) 37–55.
[59] G.V. Willingh, H.S. Abbo, S.J.J. Titinchi, Catal. Today 227 (2014) 96–104.
[60] M.R. Maurya, A. Arya, P. Adao, J.C. Pessoa, App. Catal. A: Gen. 351 (2008) 239–252.
[61] M.R. Maurya, M. Bisht, F. Avecilla, J. Mol. Catal. A Chem. 344 (2011) 18–27.
[62] D.R. Godhani, H.D. Nakum, D.K. Parmar, J.P. Mehta, N.C. Desai, Microporous Mesoporous Mater. 235 (2016) 233–245.
[63] M.R. Maurya, M. Kumar, A. Kumar, J.C. Pessoa, Dalton Trans. 28 (2008) 4220–4232.
[64] M.R. Maurya, P. Saini, A. Kumar, J.C. Pessoa, Eur. J. Inorg. Chem. 31 (2011) 4846–4861.
[65] C.K. Modi, J.A. Chudasama, H.D. Nakum, D.K. Parmar, A.L. Patel, J. Mol. Catal. A

Chem. 395 (2014) 151–161.
[66] D.R. Godhani, H.D. Nakum, D.K. Parmar, J.P. Mehta, N.C. Desai, J. Mol. Catal. A Chem. 426 (2017) 223–237.
[67] J.P. Mehta, D.K. Parmar, H.D. Nakum, D.R. Godhani, N.C. Desai, J. Porous Mater. 25 (2018) 1649–1658.
[68] C.K. Modi, R.S. Vithalania, D.S. Patela, N.N. Somb, P.K. Jha, Microporous Mesoporous Mater. 261 (2018) 275–285.
[69] N.C. Desai, J.A. Chudasama, B.Y. Patel, K.A. Jadeja, T.J. Karkar, J.P. Mehta, D.R. Godhani, Microporous Mesoporous Mater. 242 (2017) 245–255.
[70] L. Menini, M.C. Pereira, L.A. Parreira, J.D. Fabris, E.V. Gusevskaya, J. Catal. 254 (2008) 355–364.
[71] H. Wójtowicz-Młochowska, Rec. adv. Arkivoc part ii (2017) 12–58.